# Distributed OFDM Transmitter Scheme for Internet of Things

# Distributed OFDM Transmitter Scheme for Internet of Things

Yuan Ding[1], Vincent Fusco[2], Junqing Zhang[3]
[1] The Microwave and Antenna Engineering Research Group, School of Engineering and Physical Sciences, Heriot-Watt University, Edinburgh, EH14 4AS, United Kingdom (yding03@qub.ac.uk)
[2] The Institute of Electronics, Communications and Information Technology (ECIT), Queen's University Belfast, Belfast, BT3 9DT, United Kingdom
[3] Department of Electrical Engineering & Electronics, University of Liverpool, Brownlow Hill, Liverpool, L69 3GJ, United Kingdom

***Abstract*—This paper proposes a new type of distributed orthogonal frequency-division multiplexing (OFDM) transmitter architecture, which can be used in the Internet of Things (IoT) networks with distributed sensor nodes, where the nodes are required to send different data back to the hub simultaneously. The sub-carrier settings for analogue OFDM modulation across the entirety of the distributed sensor network are enabled by a broadcasted two-tone signal. The performance of the proposed two-tone sub-carrier synchronization approach is evaluated under different two-tone signal to noise ratios (SNRs). Furthermore, system bit error rates (BERs) are simulated for various sub-carrier frequency offsets and transmitter settings, in order to provide guidelines for practical system designs.**

***Keywords—bit error rate (BER); carrier synchronization; distributed transmit array; OFDM; microwave transmitter***

## I. INTRODUCTION

The Internet of Things (IoT) related products are growing at two digits per year [1] with estimations of market value in the order of trillions of dollars in the next decade [2].

At the physical layer, IoT actually employs technologies developed for the wireless sensor networks (WSNs), with a hub being replaced by an Internet access point. According to different application scenarios there are mainly two types of communication between the hub and the distributed sensor nodes. (i) When all the sensor nodes are co-operatively monitoring distributed beamforming, i.e., all the sensor nodes collaboratively steer the radiation beams towards the intended receiver, is preferred. This requires a frequency-synchronized and phase-coherent radio frequency (RF) carrier being shared among all the distributed nodes [3], [4]. (ii) On the other hand, when the nodes are monitoring different parameters, which is more common in IoT where various 'Things' are connected, then individual links between the hub and each sensor node are required. These links can be maintained in time-division duplex (TDD) or frequency-division duplex (FDD) fashion. However, in the TDD mode each sensor node has to get an agreement on time-slot assignment, or be constantly powered up waiting for an 'acquiring signal' originated from the hub. This can be problematic due to the fact that the sensors are physically distributed and power-limited. The FDD mode, on the other hand, transfers the problems to the hub node, since a bank of very narrow band, high Q filters, and most critically multiple RF chains are normally required. Against this background, in this paper we propose a new method that is able to coordinate all the sensor nodes in order to form an OFDM transmitter, which brings the following benefits:

- It can support high data rate when multiple sub-carriers are used;
- The hub design is simple. In fact, an OFDM transceiver with an FFT module and one RF chain, e.g., an IEEE 802.11 WIFI access point, can be leveraged;
- The system is scalable since adding or removing sensor nodes in the system requires only minor driver upgrades at the hub node;
- When the collected data at all sensor nodes are interleaved, the effect of deep fading between the hub and each sensor node can be alleviated.

This paper is organized as follows. In Section II the proposed two-tone distributed OFDM transmitter architecture is described. In Section III sub-carrier frequency distribution across the entire sensor network is firstly evaluated by simulation under different two-tone signal to noise ratios (SNRs). Then the system bit error rates (BERs) for different sub-carrier settings are obtained in order to guide system designs. Finally, conclusions are drawn in Section IV.

## II. TWO-TONE ENABLED DISTRIBUTED OFDM TRANSMITTER

OFDM modulation is usually performed by an IFFT module positioned in the digital baseband. However, due to the distributed nature of the sensor nodes in envisaged co-operating IoT scenarios such digital OFDM architecture is not usable. As an alternative, in this paper we propose a novel scheme, wherein an analogue OFDM with each sensor node within a distributed environment being modulated onto one designated sub-carrier is to be constructed. One critical requirement for such an analogue OFDM transmitter is the adherence to absolutely identical frequency spacing between each pair of two consecutive sub-carriers. This condition guarantees the frequency orthogonality required for

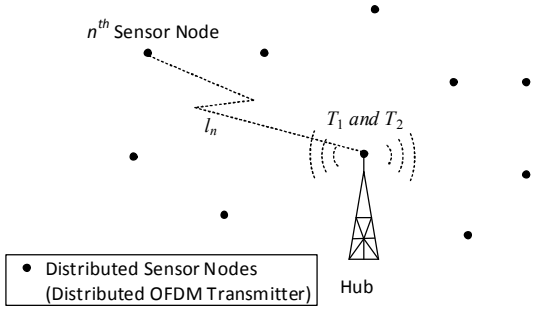


Fig. 1. Illustration of distributed OFDM transmitter.

demodulation. Importantly, since physically distributed sensor nodes that are not hard linked cannot access a common local oscillator (LO), the RF carriers synthesized locally at each sensor node are not phase locked together. Consequently, the OFDM requirement stated above is immediately violated. In order to set the correct frequency and synchronized phase for each node, a two-tone approach is proposed and is elaborated as follows;

**Step 1:** Broadcast a two-tone RF signal $T_1$ and $T_2$, which can be originated from one of the sensor node or from the hub node, see illustration in Fig. 1. The hub node is preferred since this will eliminate carrier recovery for frequency down-conversion before OFDM demodulation. The two-tone signal can be written as

$$T_1 = A\cos(2\pi f_1 t), \tag{1}$$

$$T_2 = A\cos(2\pi f_2 t+\varphi), \tag{2}$$

where A is the magnitude of the tones. $f_1$ is selected as the frequency of the first sub-carrier. The frequency separation $\Delta f$, i.e., $f_2 - f_1$, is set to the OFDM sub-carrier spacing. Since $T_1$ and $T_2$ are generated from a common LO, they are phase locked, i.e. the phase difference $\varphi$ is time-invariant.

**Step 2:** Each sensor node is equipped with two phase-locked-loops (PLLs) locking to $f_1$ and $f_2$. Their outputs are expressed as

$$O_{n1} = B\cos[2\pi f_1(t-l_n/c)], \tag{3}$$

$$O_{n2} = B\cos[2\pi f_2(t-l_n/c)+\varphi], \tag{4}$$

where $B$ is the magnitude, and $l_n$ refers to the equivalent path length between the hub node and the $n^{th}$ ($n$ = 1, 2, …, $N$) sensor node, seen in Fig. 1. $\Delta f$ is normally small enough to justify a flat-fading channel assumption used here, i.e., equivalent path lengths at both $f_1$ and $f_2$. $c$ denotes the speed of light.

**Step 3:** $O_{n1}$ and $O_{n2}$ are up-mixed at the $n^{th}$ sensor node, and after filtering out the higher frequency component, an intermediate frequency (IF) signal $IF_n$ is obtained,

$$IF_n = C\cos[2\pi\Delta f(t-l_n/c)+\varphi], \tag{5}$$

where $C$ is the magnitude.

Mathematically the required sub-carrier at the $n^{th}$ sensor node can be generated by mixing $O_{n1}$ and frequency multiplied $IF_n$ with a factor of ($n$ − 1). However, this approach can be problematic when the practical implementation is considered because the LO leakage at the frequency mixing stage requires very narrow band bandpass filters. Thus, the procedures from Step 4 to Step 6 are used.

**Step 4:** The $n^{th}$ sensor node locally synthesizes an RF carrier $T_{n3}$ at frequency $f_1+(n-1)\Delta f$, see (6),

$$T_{n3} = D\cos\{2\pi[f_1+(n-1)\Delta f]t+\theta_n(t)+\varsigma\}, \tag{6}$$

where $D$ is the magnitude. $T_{n3}$ and $T_1$ (or $T_2$) are not generated from the same LO, hence are not phase locked and a time-variant phase term between them exists, i.e., $\theta_n(t)$ . In order to simplify the formulation below the fixed phase term $\varsigma$ in (6), without loss of generality, is set to zero hereafter.

At the same time the $IF_n$ is frequency multiplied by a factor of ($n$ − 1), shown in (7),

$$S_n = C\cos[2\pi(n-1)\Delta f(t-l_n/c)+\varphi]. \tag{7}$$

**Step 5:** After mixing $T_{n3}$ and $O_{n1}$, and removing out the higher frequency component, a signal $U_n$ at the frequency $(n-1)\Delta f$ is obtained,

$$U_n = C\cos[2\pi(n-1)\Delta f t+\theta_n(t)+2\pi f_1 l_n/c]. \tag{8}$$

Summing $U_n$ and $S_n$, a signal $V_n$ with beat magnitude $\mu$ will be observed.

$$V_n = \mu\cos[2\pi(n-1)\Delta f l_n/c-\xi] \tag{9}$$

where

$$\mu = C\sqrt{2+2\cos\left\{2\pi\left[f_1+(n-1)\Delta f\right]l_n/c-\varphi+\theta_n(t)\right\}} \tag{10}$$

and

$$ctg\xi = \frac{\cos\left[2\pi(n-1)\Delta f l_n/c-\varphi\right]+\cos\left[2\pi f_1 l_n/c+\theta_n(t)\right]}{\sin\left[2\pi(n-1)\Delta f l_n/c-\varphi\right]-\sin\left[2\pi f_1 l_n/c+\theta_n(t)\right]}. \tag{11}$$

**Step 6:** Use the beat frequency observed in the magnitude $\mu$ as feedback to adjust the frequency of $T_{n3}$ until beating disappears. As a consequence, at the steady state $\theta_n(t)$ = 0, and $T_{n3}$ can be written as

$$T_{n3} = D\cos\{2\pi[f_1+(n-1)\Delta f]t\} \tag{12}$$

Equation (12) features phase-locked frequencies across the entire distributed sensor node environment, and can therefore be exploited for distributed analogue OFDM modulation.

The properties of the above presented distributed OFDM transmitter are summarized as below;

- All the filters involved in the system are low pass filters (LPFs) and can be easily designed because the in-band and out-band signals are widely separated in frequency, i.e., in-band signals are $\approx \Delta f$, out-band signals $\approx f_1+f_2$;
- The sub-carrier frequency spacing $\Delta f$ is controlled by the two-tone signal, which facilitates the OFDM sub-carrier adjustments across the entire distributed sensor nodes;
- Adding or removing sensor nodes can be readily implemented as long as sub-carrier assignments do not overlap;
- It should be pointed out that from the receiver's (the hub's) point of view the received signals in the proposed distributed analogue OFDM systems are different from the received signals when a conventional digital OFDM transmitter is used. This is because in the distributed system each sub-carrier signal experiences different propagation paths $l_n$, leading to independent amplitude attenuation and phase delays. When summing up all the sub-carriers at the receiver side, the detected signals in the time-domain look scrambled. However, when training sequences are appended at the beginning of the signal modulated to each sub-carrier, the above-mentioned amplitude and phase distortion can be fully calibrated out.

## III. Simulation Results

In this section the performance of the proposed distributed OFDM system is evaluated through simulation under various channel SNRs and system configurations. The two-tone synchronization signal is assumed to originate from the hub.

When the channel noise between the hub and the sensor nodes is considered, the output signals $O_{n1}$ and $O_{n2}$ of the two PLLs at the $n^{th}$ sensor node in (3) and (4) become

$$O_{n1} = B\cos[2\pi f_1(t-l_n/c)]+p_{n1}(t), \quad (13)$$

$$O_{n2} = B\cos[2\pi f_2(t-l_n/c)+\varphi]+p_{n2}(t), \quad (14)$$

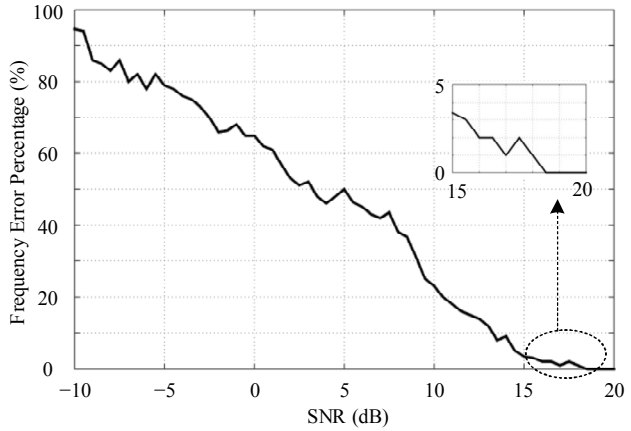


Fig. 2. Simulated frequency error percentage versus two-tone SNR. $f_1$ = 2403.9 MHz, $\Delta f$ = 312.5 kHz, and $\theta(t) = 1\times10^5 t$.

here noise $p_{n1}(t)$ and $p_{n2}(t)$ are modelled as independent additive white Gaussian noise (AWGN) with a mean of zero and identical power spectral density of $N_0/2$. Since a PLL has the ability of suppressing input noise beyond its loop bandwidth [5], the model used in (13) and (14) can be considered to represent the worst cases.

Noise $p_{n1}(t)$ and $p_{n2}(t)$ contaminate the beat frequency, denoted as $f_b$, observed in the magnitude of $V_n$ in (9), and hence affect the phase locking between the $T_{n3}$ and the $O_{n1}$. The frequency error percentage, defined as

$$E_f = [f_b-\theta(t)/t]/[\theta(t)/t]\times100\%, \quad (15)$$

for various SNRs was obtained through Monte Carlo simulation and is presented in Fig. 2. In simulation $l_n$ is randomly selected in the range from 5 $m$ to 10 $m$, and $f_1$ and $\Delta f$ are, respectively, set as 2412−20/64×26 = 2403.9 MHz and 20/64 = 0.3125 MHz, which are used in IEEE 802.11 standard (Channel 1 in 2.4 GHz band) [6]. $\theta(t)$ is assumed to be $1\times10^5 t$. In addition, a five-order Butterworth LPF, designed with a cutoff frequency 5 MHz, was used to select the required IF signals at around $\Delta f$. From Fig. 2 it can be observed that the frequency error percentage converges towards zero when the detected two-tone SNR approaches 20 dB.

Before investigating the impact of the frequency errors on the system performance, the bit error rates (BERs) in ideal distributed OFDM systems, i.e., $E_f$ = 0, were simulated for various transmitter configurations. $10^{+6}$ random data bits modulated for both QPSK and 16QAM were generated and used in simulation. The standard IEEE 802.11 OFDM physical layer protocol [6] is adopted, including frequency sub-carrier assignment (64 sub-carriers evenly spread in 20 MHz channel spacing and channel 1 in 2.4 GHz band) and data packet configuration. It has been found in the results shown in Fig. 3 that the number of the sensor nodes $N$, which equals the number of the occupied data sub-carriers, and the frequency separations among them, $k\Delta f$ ($k$ is an integer), have no effect on the system performance. This is because with no frequency error the sub-carriers are perfectly orthogonal to each other. Furthermore, importantly, the simulated BER results follow the

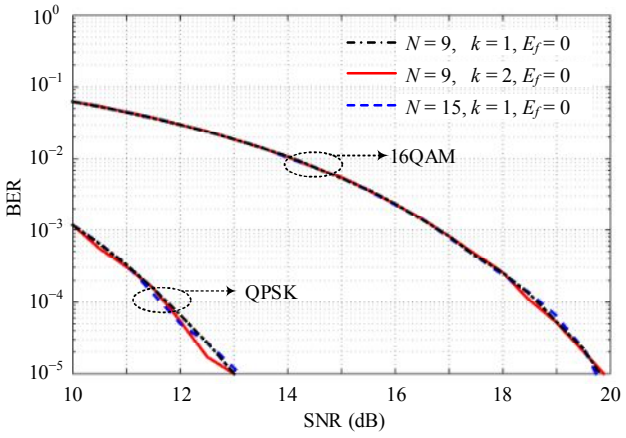


Fig. 3. Simulated BER performance in ideal $E_f$ = 0 analogue distributed OFDM systems for different transmitter configurations. $l_n$ is randomly selected in the range from 5 $m$ to 10 $m$. $10^{+6}$ random bits were used in simulation.

classic BER-SNR curves [7], indicating no performance difference between the conventional digital IFFT-based and the proposed, in its ideal form, analogue distributed OFDM transmitter assembly. It needs to be pointed out that the SNR in Fig. 3, as well as shown in Fig. 4 and Fig. 5, describe the cumulative signal quality at the hub, while the SNR in Fig. 2 refers to the two-tone signal at each sensor node. They are different.

Next the impact of the frequency errors that could exist in distributed systems on achievable BERs is investigated.

Simulation results for QPSK and 16QAM cases are presented in Fig. 4 and Fig. 5, respectively. As expected, higher frequency errors lead to increased BER. The results presented in Figs. 4 and 5 can provide a guideline for data coding design.

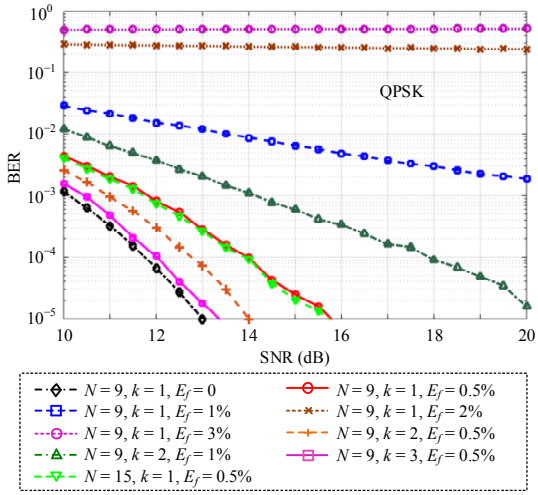


Fig. 4. Simulated BER performance in example analogue distributed OFDM systems for different transmitter configurations. $10^{+6}$ random bits modulated for QPSK were used in simulation.

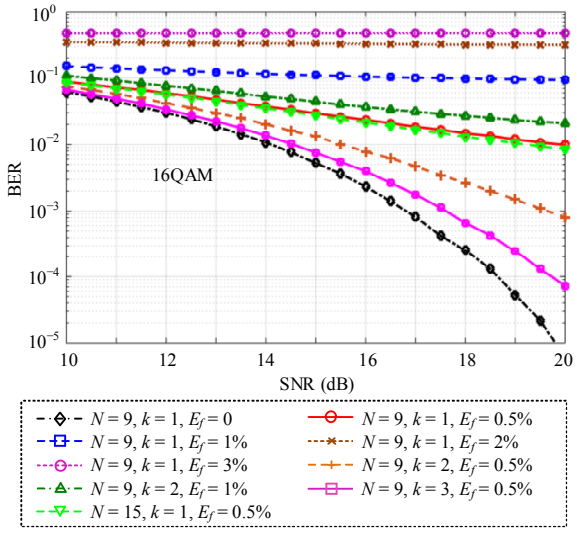


Fig. 5. Simulated BER performance in example analogue distributed OFDM systems for different transmitter configurations. $10^{+6}$ random bits modulated for 16QAM were used in simulation.

Lower code rates are required for error correction when frequency errors in the distributed OFDM systems are relatively higher. Also intuitively, for a fixed frequency error, wider frequency spacing (greater the $k$ used in simulation) between occupied sub-carriers helps alleviate the negative impact of frequency error on BER. It is noted that the number of distributed sensors does not affect the BER as long as it is less than the number of data sub-carriers, e.g., 48 in IEEE 802.11, which can also be observed in Fig. 4 and Fig. 5.

## IV. Conclusions

In this paper a two-tone enabled distributed analogue OFDM transmitter architecture was presented. The two-tone signal broadcasted wirelessly from a reference node was frequency mixed at each sensor node. The obtained IF signals were utilized to set phase-locked OFDM sub-carriers at each distributed node. The performance of the phase-locking, described by frequency errors, and system BERs were simulated under different channel SNRs and transmitter settings. The proposed distributed OFDM system should prove useful to distributed IoT networks where the nodes are required to send different data back to the hub simultaneously.

## Acknowledgment

This work was supported by the EPSRC (UK) under Grants EP/N020391/1 and EP/P000673/1. The authors thank the funding support from the School of Engineering and Physical Sciences, Heriot-Watt University.

## References

[1] L. Roselli, N. Borges, F. Alimenti, P. Mezzanotte, G. Orecchini, M. Virili, C. Mariotti, R. Goncalves, and P. Pinho, "Smart surfaces: large area electronics systems for Internet of Things enabled by energy harvesting," IEEE Proc., vol.102, no.11, pp.1723-1746, Nov. 2014.

[2] J. Manyika, M. Chui, J. Bughin, R. Dobbs, P. Bisson, and A. Marrs, "How the Internet of Things is more like the Industrial Revolution than the Digital Revolution," MGI Rep., 2013. [Online]. Available: http://www.mckinsey.com/insights/business_technology/disruptive_technologies

[3] R. Mudumbai, D. R. Brown, U. Madhow, and H. V. Poor, "Distributed transmit beamforming: challenges and recent progress," IEEE Commun. Mag., vol. 47, no. 2, pp. 102-110, Feb. 2009.

[4] N. Xie, X. Bao; A. Petropulu, and H. Wang, "Fast open-loop synchronization for cooperative distributed beamforming," in Proc. IEEE Global Telecommun. Conf., Dec. 2013, pp. 3441-3446.

[5] F. A. Musa, "Noise analysis of phase locked loops and system trade-offs," [Online]. Available: http://www.eecg.toronto.edu/~kphang/papers/2002/fmusa_pllnoise.pdf

[6] Wireless LAN Medium Access Control (MAC) and Physical Layer (PHY) Specification, IEEE Std. 802.11, 2012.

[7] R.A. Shafik, S. Rahman and A. R. Islam, "On the extended relationships among EVM, BER and SNR as performance metrics," in Proc. Int. Conf. on Electrical and Computer Engineering, pp. 408-411, 2006.